Advanced glycation end products and their related signaling cascades in adult survivors of childhood Hodgkin lymphoma: A possible role in the onset of late complications

Advanced glycation end products and their related signaling cascades in adult survivors of childhood Hodgkin lymphoma: A possible role in the onset of late complications

Francesco Felicetti [a 1], Eleonora Aimaretti [b 1], Federica Dal Bello [c], Filippo Gatti [a], Alessandro Godono [d], Francesca Saba [e], Giacomo Einaudi [f], Massimo Collino [g], Franca Fagioli [d h], Manuela Aragno [b 1], Enrico Brignardello [a 1*]

[a]Transition Unit for Childhood Cancer Survivors, Città della Salute e della Scienza Hospital, Turin, Italy
[b]General Pathology Unit, Department of Clinical and Biological Sciences, University of Turin, Turin, Italy
[c]Department of Molecular Biotechnology and Health Sciences, University of Turin, Italy
[d]Department of Public Health and Pediatrics, University of Torino, Turin, Italy
[e]Department of Medical Science, University of Turin, Turin, Italy
[f]Pharmacology Unit, School of Pharmacy, University of Camerino, Camerino, Italy
[g]Department of Neurosciences "Rita Levi Montalcini" University of Turin, Turin, Italy
[h]Division of Paediatric Onco-Haematology, Stem Cell Transplantation and Cellular Therapy, Città della Salute e della Scienza Hospital, Turin, Italy

* Corresponding author. Transition Unit for Childhood Cancer Survivors, A.O.U. Città della Salute e della Scienza di Torino, Corso Bramante 88, 10126, Torino, Italy.
E-mail addresses: ebrignardello@cittadellasalute.to.it, unitaditransizione@cittadellasalute.to.it (E.Brignardello).

1 Equally contributed to this work.

Abstract

Hodgkin lymphoma (HL) is today one of the most curable pediatric cancers. Despite survival rates now exceeding 90%, survivors of pediatric HL are still at higher risk to develop late effects of cancer therapy. Premature aging has been proposed as a paradigm to explain the onset of long-term complications in these subjects. High levels of advanced glycation end products (AGEs), together with chronic inflammation and oxidative unbalance, have been shown to be among the main factors contributing to aging. The present study aims to evaluate glycoxydation, inflammatory status, and oxidative stress in plasma and peripheral blood mononuclear cells (PBMC) obtained from 20 adult survivors of pediatric HL and 40 age- and sex-matched healthy controls. After the isolation of PBMC and the collection of plasma, we performed the analyses of gene expression by qRT-PCR and measured inflammatory and oxidative-stress markers. AGEs plasma levels, expressed as Nϵ-carboxymethyl-lysine and methylglyoxal hydroimidazolone, were markedly higher in HL survivors than in healthy subjects. HL survivors also showed a condition of higher oxidative stress, as demonstrated by an increased expression of NADPH oxidase on PBMC. Antioxidant defenses, evaluated in terms of alpha-tocopherol, GSSG/GSH ratio and catalase plasma levels, were strongly impaired in survivors. This pro-oxidative condition led to the over-expression of both NLRP3 and NFkB genes in PBMC and, consequently, to increased plasma levels of interleukin(IL)-1β and IL-6. Finally, the expression of the receptors for AGEs in PBMC confirmed the dysregulated AGE pathways.

Data show AGEs accumulation in survivors of pediatric HL. The consequent activation of the receptor for AGEs leads to the persistent activation of intracellular signaling toward inflammation. These results suggest that the co-existence of AGEs accumulation, unbalanced oxidative status, and inflammation could play a role in the onset of late complications in HL survivors.

Highlights

- Survivors of pediatric Hodgkin lymphoma have higher AGEs plasma levels than controls.
- Survivors show higher oxidative stress and impaired antioxidant defenses.
- NLPR3 and NFkB genes are overexpressed in PBMC of survivors.
- AGEs accumulation could represent the “metabolic memory” of anticancer treatments.

Keywords: Advanced glycation end products; RAGE; Oxidative stress; Inflammation; Late effects; Hodgkin lymphoma.

1. Introduction

Thanks to the use of modern treatment protocols, Hodgkin lymphoma (HL) is now one of the most curable pediatric cancers with survival rates today exceeding 90% [1].
Even if cured, survivors of pediatric HL are at higher risk of developing late effects of cancer therapy that can impact on their quality of life and even limit life expectancy over time [2,3]. Compared with the general population, survivors of childhood HL show a 5.1-fold higher risks of death due to cause other than HL [4], cardiovascular disease, and second malignant neoplasms accounting for about 2/3 of this mortality excess [4]. Although the biological and molecular mechanisms underlying the onset of late effects in childhood cancer survivors are still debated, premature aging has been proposed as a paradigm to explain the onset of long-term complications in these subjects [5]. At age 54 HL survivors show the same cumulative mortality (20%) as 71-year-old individuals from the general population [4], and there is evidence that they are at risk of early onset of aging. Survivors of childhood HL - as well as survivors of any other childhood cancer - were indeed exposed to potentially damaging agents that may have affected tissue integrity, cellular function, and DNA structure, leading to premature activation of the molecular processes usually seen in older adults.
High levels of advanced glycation end products (AGEs) have been shown to be one of the main factors contributing to aging [6,7]. AGE are a heterogeneous group of molecules formed by non-enzymatic reactions of reducing sugars with amino acids of proteins, lipids, and nucleic acids [8]. Our recent report showing a marked increase of AGEs plasma levels in adult survivors of pediatric acute lymphoblastic leukemia who had received chemotherapy and allogeneic hematopoietic stem cell transplantation conditioned with total body irradiation, compared with the normal population, fits with this scenario [9]. Chronic inflammation and oxidative unbalance may also contribute to premature aging and to the pathogenesis of late effects in cancer survivors [5,9,10].
The present study aims to evaluate glycoxydation, inflammatory status, and oxidative stress in plasma and peripheral blood mononuclear cells (PBMC) obtained from adult survivors of pediatric HL and healthy controls.

2. Material and methods

2.1. Subjects

Among patients routinely followed at the Transition Unit for Childhood Cancer Survivors at Città della Salute e della Scienza Hospital in Turin, 20 consecutive HL survivors were enrolled in the study.
Inclusion criteria were: (a) previous diagnosis of Hodgkin Lymphoma at age <25 years; (b) age at the time of the enrollment >18 and < 40 years; (c) have been off-therapy for >5 years.
HL survivors who received allogeneic HSCT were excluded. Moreover, glucose metabolism alterations (diabetes mellitus or impaired fasting glucose), BMI >25, smoking (active or stopped for less than one year), ongoing illness, and active treatment with anti-inflammatory (steroidal as well as non-steroidal) or other potentially interfering drugs were considered as exclusion criteria.
For the purpose of this study, 40 healthy volunteers were enrolled among Città della Salute e della Scienza Hospital employees, during periodical occupation medicine evaluations.
The study was approved by the Ethics Committee of the Hospital (no. CS2/1174), and all included subjects have signed the informed consent.

2.2. Plasma separation

Blood samples were collected after a fasting period of at least 8 h in EDTA tubes. Plasma, obtained following a 15 min centrifugation at 1500 RPM, was then stored at −80 °C.

2.3. Peripheral blood mononuclear cells (PBMC) extraction

PBMC were extracted from whole blood using Ficoll (Ficoll-Paque Plus, GE Healthcare Europe GmbH, Germany) and gradient centrifugation (1400 RPM, RT for 35 min), which separate the blood cells into a top layer of plasma, an intermediate layer of PBMC, and a bottom fraction of polymorphonuclear cells and erythrocytes.
After isolation, PBMC were washed twice with 0.9% saline solution, suspended in 0.5 mL of TRIzol reagent (Sigma-Aldrich, St. Louis, MO 63103, USA) and stored at −80 °C. After resuspension of PBMC, 0.2 mL of chloroform per 1 mL of TRIzol Reagent were added and, following a 15 min centrifugation at 12000 RPM, the mixture was separated and the upper aqueous phase transferred into fresh tubes. The total ribonucleic acid (RNA) was precipitated from the aqueous phase by mixing it with isopropyl alcohol and centrifuged at 12000 RPM for 15 min. The RNA pellet was washed twice with 75% ethanol, air-dried for 10–15 min, suspended in RNA-ase/DNA-ase free water, and then stored at −80 °C.

2.4. Plasma analyses

High-sensitivity C-reactive protein (hs-CRP) was measured with a nephelometric method, following the manufacturer's instructions. sRAGE levels were determined using a double-sandwich ELISA kit (DuoSet ELISA development kit; R&D Systems, Minneapolis, MN, USA) following the manufacturer's instructions for absorbance reading. Interleukin (IL)-6 (Abcam, ab178013, Human IL-6 ELISA kit) and IL-1β (R&D Systems Inc, Quantikine ELISA Human IL-1β/IL-1F2 Immunoassay, Minneapolis MN, USA) were quantified with ELISA kits following the manufacturer's instructions.
Catalase activity (Abcam, ab83464, Catalase Activity Assay kit) was measured colorimetrically following the manufacturer's instructions.
GSSG/GSH ratio was quantified with the Oxiselect Total Glutathione (GSSG/GSH) Assay Kit (Cell Bio-labs Inc, San Diego, CA) following the manufacturer's instructions for kinetic reading.

α-tocopherol was analysed and quantified by a LCMS-8045 (Shimadzu) instrument. Aliquots of 300 µL of a mixture of ethanol/acetonitrile (44/56) were added to 50 µL of samples. After vortexing and centrifugation at 1600*g* × 10 min, 4 °C, the supernatant was dried in a CentriVap Centrifugal Vacuum Concentrators (Labconco Corporation, Kansas City, MO, USA) and reconstituted before UHPLC-MRM analysis with 100 µL of aqueous 0.1% formic acid/acetonitrile (50/50).
The chromatographic separation was achieved using a reverse phase C18 column (Luna(2) 150 × 3.0 mm, 3.0 µm particle size, Phenomenex) at a flow rate of 0.30 µL/min in isocratic mode with a column temperature of 40 °C. The eluent composition was methanol 100% and the injection volume was 20 µL. Retention time of α-tocopherol was 10.7 min. The LC column eluent was delivered to the ESI source using nitrogen as nebulizing (3 L/min) and drying (10 L/min) gas. ESI negative interface voltage was set to −3.0 kV; temperatures of desolvation line and of heat block were 250 and 400 °C, respectively. The MRM transition for the vitamin E analysis was 429@163 with a collision energy of 30 V (argon was used as collisional gas) and the potentials applied on the quadrupoles were 12 V for Q1 and 29 V for Q3. Quantitative determination was done by using vitamin E analytical standards calibration curves.

3. AGE levels in plasma

Nϵ-carboxymethyl-lysine (CML) was measured by ultra-high-performance liquid chromatography (UHPLC)-tandem mass spectrometry. In brief, 50 µL of sample were hydrolyzed with 500 µL of 0.6 M trichloroacetic acid and 50 mL of 6 M hydrochloric acid for 2 h at 60 °C. The analyses were performed on a UHPLC coupled to a triple quadrupole mass spectrometer (AB-Sciex Triple Quad 5500, Milan, Italy), equipped with a Turbo ion ESI source. Analytes were separated on a reversed-phase C18 column (Kinetex 100 × 2.1 mm, 1.7 µm particle size, Phenomenex) at a flow rate of 0.35 µL min−1. A gradient mobile phase composition of 95/5–40/60 over 25 min in 5 nM heptafluorobutanoic acid/acetonitrile was adopted. The liquid chromatograph column eluent was delivered to the Turbo ion source using nitrogen as a sheath (GS1) and curtain (CUR) gas, and air as reagent gas (GS2).
The source voltage was set at 4.5 kV in positive mode, CUR 26 arbitrary units (arb), GS1 45 arb, and GS2 50 arb. The heated capillary was maintained at 275 °C. The MRM transitions and parameters were as follows: Nϵ-(carboxymethyl)-lysine (*m*/*z*) 205@84, declustering potential (DP) 100 V, entrance potential (EP) 7 V, collision energy (CE) 32 V. Quantification of analytes was performed using CML standard calibration curve at concentrations of 10, 50, 100, 250, 300, and 500 µg L−1. Measured concentration of analytes in samples was always within the linear range of calibration. Coefficient of variation for the above analyses ranged from 8% to 14%.
Methylglyoxal hydroimidazolone (MG-H1) was analysed and quantified with a LCMS-8045 (Shimadzu) instrument using MGH1-d3 deutered standard as internal standard. For sample preparation, 50 µL of plasma matrix were hydrolyzed with 500 µL of 0.6 M trichloroacetic acid and 50 mL of 6 M hydrochloric acid for 2 h at 60 °C. Internal standard was added before the acid hydrolysis at concentration of 150 ng/mL. The chromatographic separations were run on a reversed phase C18 column (Luna C18(2) 150 × 3.0 mm, 3.0 µm particle size, Phenomenex) and flow rate and injection volume were 0.25 µL/min and 3 µL respectively. We used for the chromatographic separation 0.1% of formic acid aqueous solution (A) and acetonitrile (B) and the gradient run composition changed from 95/5 (A/B) to 0/100 (A/B) in 15min. Then the column went back to the initial condition. The column oven was maintained at 40 °C. The LC column eluent was delivered to the ESI source using nitrogen as nebulizing (3 L/min) and drying (10 L/min) gas. The source voltage was set at 4.0 kV in the positive mode; the heat block temperature was maintained at 400 °C. The MRM transitions and parameters were as follows:
- MG-H1 (*m*/*z*) 229@70, CE 25.0 and the potentials applied on the quadrupoles were 21 V for Q1 and 25 V for Q3;

- MG-H1-d3 (*m*/*z*) 232@117, CE 14.0 and the potentials applied on the quadrupoles were 11 V for Q1 and 21 V for Q3.
MG-H1 was analysed and quantified with a LCMS-8045 (Shimadzu) instrument using MG-H1-d3 deutered standard as internal standard.

3.1. Western blot

Proteins were separated by 10%–12% sodium dodecyl sulphate-polyacrylamide gel electrophoresis (SDS-PAGE) and transferred to a polyvinyldenedifluoride (PVDF) membrane, which was then incubated over-night with primary antibodies (dilution 1:1000). The antibodies used were purchased by Cell Signalling Technology (#15101 NLRP3; #39754 Gasdermin D; #8242 NF-κB p65; #4301 p47phox). The blots were then incubated with anti-rabbit secondary antibodies conjugated with horseradish peroxidase (dilution 1:10000) and developed using an ECL detection system. Bio-Rad Image Lab Software 6.0.1 was used to analyze the immunoreactive bands and the results were normalized to GAPDH (Cell Signalling Technology, #5174).

3.2. PBMC analyses

RNA was retrotranscripted using the SensiFAST cDNA Synthesis Kit 50 Reactions kit (BIO-65053, Bioline GmbH, Germany). SensiFAST™ SYBR® No-ROX Kit 500 reactions (BIO-98005, Bioline GmbH, Germany) was used for quantitative real-time polymerase chain reaction (qRT-PCR). Relative gene expression was obtained after normalization to housekeeping genes β-actin and β-2-microglobulin using formula 2-ΔΔCT. The primers listed in the following from Qiagen SRL were used: beta-actin (QT01680476), beta-2-microglobulin (QT00088935), interleukin 6 (QT00083720), advanced glycosylation end product-specific receptor (AGE-R) (QT00000119), NADPH oxidase 1 (NOX-1) (QT00025585), NLR family, pyrin domain containing 3 (NRLP3) (QT01666343), p65/RELA (QT01007370), interleukin 1β (QT00021385), AGER1/DDOST (OST-48) (QT00081466), gasdermin-D (GSDMD) (QT01155448). Negative controls for reverse transcription (no reverse transcriptase enzyme) and for qPCR (no complementary deoxyribonucleic acid) were included in the experiments.

3.3. Statistical analysis

Data are expressed as mean ± S.E.M. (standard error of mean), and calculations were performed using GraphPad Prism 7. Unless otherwise stated, statistically significant differences between groups were assessed by Student *t*-test to determine if there was a significant difference between the means of the two groups. Outliers were detected by ROUT (robust regression and outlier removal) method, Q = 1.0% (GraphPad 7). The statistically significant level was set at $p < 0.05$.

4. Results

Demographic data and clinical characteristics of HL survivors are summarized in Table 1. Plasma levels of CRP, IL-1β and IL-6 were significantly higher in HL survivors than in the controls (Table 2). Compared to controls, HL survivors also exhibited lower plasma levels of α-tocopherol (Fig. 1, panel A; $p < 0.05$), an increased GSSG/GSH ratio (Fig. 1, panel B; $p < 0.05$), and markedly higher catalase activity (Fig. 1, panel C; $p < 0.05$). Taken together, these results indicate inflammation, antioxidants consumption, and activation of antioxidant enzymes. In PBMC of HL survivors, the gene expression of NAPDH-oxidase was about doubled than in the controls (Fig. 2, panel A; $p < 0.01$). This enzyme transports electrons across the plasma membrane and generates superoxide and other downstream ROS. Dysregulated redox signaling and oxidative injury are associated with inflammatory processes. A higher gene expression of p65 (one of the five

components that form the NF-κB), NLRP3 inflammasome (a multiprotein complex that orchestrates several pathways involved in the maturation of the inflammatory cytokine pro-IL-1β), and GSDM-D (which cooperate in triggering the release of inflammatory cytokines and pyroptosis) were observed in the PBMC of HL survivors (Fig. 2, panel B, C and D, respectively). The evaluation of inflammatory and oxidative stress markers using western blot analysis confirmed these results (Fig. 3). The presence of an active inflammatory status in HL survivors is also confirmed by the higher expression of IL-1β (Fig. 4, panel A; $p < 0.0001$) and IL-6 genes (Fig. 4, panel B; $p < 0.05$).
The interaction between oxidative stress and inflammation induces AGEs formation. The plasma levels of CML (a major AGE compound, produced by the Maillard reaction; Fig. 5, panel A) and MG-H1 (mainly generated through highly reactive α-dicarbonyls; Fig. 5, panel B) were higher in HL survivors than in the controls (CML: 373.80 ± 41.16 μg/mL vs 250.30 ± 17.51 μg/mL, $p < 0.01$; MG-H1: 12.73 ng/mL ± 5.43 vs 3.56 ± 0.61 ng/mL, $p < 0.05$). Moreover, soluble RAGE (sRAGE), a circulating form of RAGE acting as a ligand decoy which attenuates RAGE signaling, was significantly higher in HL survivors than in controls (Fig. 5, panel C; $p < 0.05$).
The gene expression of RAGE was higher in HL survivors than in the controls (Fig. 6, panel A; $p < 0.01$), according to RAGE involvement in the induction of oxidative stress through the activation of NADPH-oxidase. By contrast, AGE receptor 1 (AGE-R1)/OST-48 gene expression was downregulated (Fig. 6, panel B; $p < 0.01$), suggesting a reduced AGER-1/RAGE ratio and a consequent impaired protection against oxidative stress in HL survivors.

5. Discussion

Our results indicate that, five years or more after the end of cancer therapies, adult survivors of pediatric Hodgkin lymphoma show higher plasma levels of CML, MG-H1, and activation of the AGE/RAGE axis. The activation of AGE/RAGE pathway is associated with oxidative unbalance and low-grade chronic inflammation. Indeed, our HL survivors had lower plasma levels of alpha tocopherol and a higher GSSG/GSH ratio, indicating a reduced activity of antioxidant defense. Moreover, compared to controls, HL survivors show a higher expression of NADPH oxidase gene, leading to ROS overproduction. HL survivors also had higher plasma levels of the inflammatory markers hs-PCR, IL-1β and IL-6. Interestingly, we also detected a higher gene expression of IL-1β and IL-6 in PBMC when compared to controls, thus confirming a local activation of inflammatory immune cells. Besides, our results show that this excessive inflammatory response is due at least in part to intracellular overactivation of two pivotal inflammatory pathways: the NfkB and NLRP3 inflammasome cascades, as confirmed by the higher expression of p65 and NLPR3 and GSDM-D genes, respectively.
These alterations, likely due to previous anticancer treatments, could play a key role in the pathogenesis of late effects in childhood cancer survivors. It is well known that ROS are promptly and greatly generated by exposure to radiotherapy and chemotherapy agents such as anthracyclines and alkylating agents [[11], [12], [13]]. The high levels of ROS rapidly induces the production of AGEs [14,15] which in turn, by interaction with RAGE, triggers the generation of ROS and the up-regulation of inflammatory pathways [14].
Recent studies on NLRP3 inflammasome show that AGEs can activate the NLRP3 inflammasome complex via oxidative and inflammatory stress [16,17]. An initial signal regulated by NFkB, for the transcription of NLRP3, is followed by a second signal that assembles the NLRP3 inflammasome, leading to an increased production of inflammatory cytokines. Moreover, the interaction of AGEs with RAGE activates NADPH oxidase, perpetuating a vicious cycle of ROS production and stimulation of NFkB (i.e., inflammation). By contrast, the binding of AGEs to the cell surface receptor AGER1 led to the inhibition of AGE- and RAGE-induced NF-κB activity, suggesting that AGER1 may mitigate AGE-induced cellular toxicity [18]. Besides, AGER1 has been shown to play a role in AGE clearance by mediating enhanced AGE uptake and degradation, with the following reduction in AGEs accumulation and RAGE activation, thus resulting in decreased ROS generation

and inflammation. Thus, AGEs accumulation could represent the fulcrum of a vicious circle perpetuating the generation of oxidative stress and inflammation firstly induced by chemotherapy and radiotherapy. A similar mechanism has been postulated to explain the "vascular glycemic memory", or "metabolic memory", in diabetic patients [19].
The combination of AGEs accumulation, persistent inflammation, and oxidative unbalance that we found in our survivors of pediatric HL may have relevance for all childhood cancer survivors. Indeed, cardiovascular diseases and second malignant neoplasms, which are the late effects mainly responsible for the mortality excess observed in CCS, are both related to chronic inflammation and oxidative stress.
Regulating the intracellular ROS levels to efficiently kill cancer cells and reduce the side effect of chemo-/radiotherapy is currently considered one of the major means of cancer treatment [20]. Our results fit with this strategy and pave the way for studies aimed to prevent the onset of post-treatment complications in (childhood) cancer survivors through the reduction of AGEs accumulation.

Declaration of competing interest: None

Funding sources

The work was supported by CRT Foundation [Complicanze tardive in giovani adulti curati per linfoma di Hodgkin in età pediatrica: ruolo dei prodotti di glicazione avanzata". Grant number RF 2019.0889, SDD Unità di Transizione per Neoplasie Curate in Età Pediatrica] and by University of Turin, Ricerca Locale 2018. The funding sources had no involvement in study design, data collection, analysis or interpretation, in the writing of the report, and in decision to submit the article for publication.

REFERENCES

[1] SEER Cancer Statistics Review, 1975-2018, National Cancer Institute, Bethesda, MD, April 2021 based on November 2020 SEER data submission, posted to the SEER web site, https://seer.cancer.gov/csr/1975_2018/.

[2] M. Cepelova, J. Kruseova, A. Luks, et al., Accelerated atherosclerosis, hyperlipoproteinemia and insulin resistance in long-term survivors of Hodgkin lymphoma during childhood and adolescence, Neoplasma 66 (6) (2019) 978–987, https://doi.org/10.4149/neo_2019_190115N45.

[3] D.C. Hodgson, Hodgkin lymphoma: the follow-up of long-term survivors, Hematol. Oncol. Clin. N. Am. 22 (2) (2008) 233, https://doi.org/10.1016/j. hoc.2008.01.004.

[4] S. de Vries, M. Schaapveld, C.P.M. Janus, et al., Long-term cause-specific mortality in Hodgkin lymphoma patients, J. Natl. Cancer Inst. 113 (6) (2021) 760–769, https://doi.org/10.1093/jnci/djaa194.

[5] K.K. Ness, J.L. Kirkland, M.M. Gramatges, et al., Premature physiologic aging as a paradigm for understanding increased risk of adverse health across the lifespan of survivors of childhood cancer, J. Clin. Oncol. 36 (21) (2018) 2206–2215, https:// doi.org/10.1200/JCO.2017.76.7467.

[6] I. Sadowska-Bartosz, G. Bartosz, Effect of glycation inhibitors on aging and agerelated diseases, Mech. Ageing Dev. 160 (2016) 1–18, https://doi.org/10.1016/j. mad.2016.09.006.

[7] M. Fournet, F. Bont´e, A. Desmouli`ere, Glycation damage: a possible hub for major pathophysiological disorders and aging, Aging Dis. 9 (5) (2018) 880–900, https:// doi.org/10.14336/AD.2017.1121.

[8] M.W. Poulsen, R.V. Hedegaard, J.M. Andersen, B. de Courten, S. Bügel, J. Nielsen, L.H. Skibsted, L.O. Dragsted, Advanced glycation endproducts in food and their effects on health, Food Chem. Toxicol. 60 (2013 Oct) 10–37, https://doi.org/ 10.1016/j.fct.2013.06.052.

[9] F. Felicetti, A.S. Cento, P. Fornengo, et al., Advanced glycation end products and chronic inflammation in adult survivors of childhood leukemia treated with hematopoietic stem cell transplantation, Pediatr. Blood Cancer 67 (3) (2020), e28106, https://doi.org/10.1002/pbc.28106.

[10] J. Sulicka-Grodzicka, A. Surdacki, M. Seweryn, et al., Low-grade chronic inflammation and immune alterations in childhood and adolescent cancer survivors: a contribution to accelerated aging? Cancer Med. 10 (5) (2021) 1772–1782, https://doi.org/10.1002/cam4.3788.

[11] E.I. Azzam, J.P. Jay-Gerin, D. Pain, Ionizing radiation-induced metabolic oxidative stress and prolonged cell injury, Cancer Lett. 327 (1–2) (2012) 48–60, https://doi. org/10.1016/j.canlet.2011.12.012.

[12] D. Cappetta, A. De Angelis, L. Sapio, et al., Oxidative stress and cellular response to doxorubicin: a common factor in the complex milieu of anthracycline cardiotoxicity, Oxid. Med. Cell Longev. 2017 (2017) 1521020, https://doi.org/ 10.1155/2017/1521020.

[13] B. Perillo, M. Di Donato, A. Pezone, et al., ROS in cancer therapy: the bright side of the moon, Exp. Mol. Med. 52 (2) (2020) 192–203, https://doi.org/10.1038/ s12276-020-0384-2.

[14] R. Ramasamy, S.J. Vannucci, S.S. Yan, K. Herold, S.F. Yan, A.M. Schmidt, Advanced glycation end products and RAGE: a common thread in aging, diabetes, neurodegeneration, and inflammation, Glycobiology 15 (7) (2005) 16R–28R, https://doi.org/10.1093/glycob/cwi053.

[15] G. Palanissami, S.F.D. Paul, RAGE and its ligands: molecular interplay between glycation, inflammation, and hallmarks of cancer-a review, Horm Canc. 9 (5) (2018) 295–325, https://doi.org/10.1007/s12672-018-0342-9.

[16] W.J. Yeh, H.Y. Yang, M.H. Pai, C.H. Wu, J.R. Chen, Long-term administration of advanced glycation end-product stimulates the activation of NLRP3 inflammasome and sparking the development of renal injury, J. Nutr. Biochem. 39 (2017) 68–76, https://doi.org/10.1016/j.jnutbio.2016.09.014.

[17] X. Deng, W. Huang, J. Peng, et al., Irisin alleviates advanced glycation end products-induced inflammation and endothelial dysfunction via inhibiting ROSNLRP3 inflammasome signaling, Inflammation 41 (1) (2018) 260–275, https://doi. org/10.1007/s10753-017-0685-3.

[18] C. Lu, J.C. He, W. Cai, H. Liu, L. Zhu, H. Vlassara, Advanced glycation endproduct (AGE) receptor 1 is a negative regulator of the inflammatory response to AGE in mesangial cells, Proc. Natl. Acad. Sci. U. S. A. 101 (32) (2004) 11767–11772, https://doi.org/10.1073/pnas.0401588101.

[19] A. Ceriello, M.A. Ihnat, J.E. Thorpe, Clinical review 2: the "metabolic memory": is more than just tight glucose control necessary to prevent diabetic complications? J. Clin. Endocrinol. Metab. 94 (2) (2009) 410–415, https://doi.org/10.1210/ jc.2008-1824.

[20] G. Huang, S.T. Pan, ROS-mediated therapeutic strategy in chemo-/radiotherapy of head and neck cancer, Oxid. Med. Cell Longev. 2020 (2020) 5047987, https://doi. org/10.1155/2020/5047987.

Table 1. Demographic and clinical characteristics of HL survivors and Controls.

	HL survivors	**Controls**	**p**
Sex (M:F)	10:10	21:19	0,855
Age at the study (years)[a]	29,6 ± 5,1	27,8 ± 4,1	0,148
Body Mass Index	21,8 ± 2,5	21,9 ± 2,5	0,867
Age at cancer diagnosis (years)[a]	12,6 ± 3,9		
Follow-up time from cancer diagnosis (years)[a]	16,0 ± 7,0		
Chemotherapy			
COPP/ABV	*13 (65,0%)*		
ABVD	*2 (10,0%)*		
Others	*5 (25,0%)*		
Radiotherapy			
Cervical (any field)	*6 (30,0%)*		
Mediastinal (any field)	*20 (100%)*		
Abdominal (any fiedl)	*5 (25,0%)*		

[a](mean ± SD).

Table 2. Inflammatory parameters (mean ± SEM) in plasma of HL survivors and Controls.

Empty Cell	**Controls**	**HL survivors**	**P**
C – reactive protein (mg/L)	0.47 ± 0.04	1.23 ± 0.31	0.005
Interleukin-1β (pg/mL)	1.02 ± 0.18	2.33 ± 0.63	0.033
Interleukin-6 (pg/mL)	5.56 ± 0.38	11.09 ± 2.33	0.034

Fig. 1. Unbalanced oxidative status. Levels of α-tocopherol (A), GSSG/GSH ratio (B) and catalase activity (C) in plasma of HL survivors and Controls. *p <
0.05.

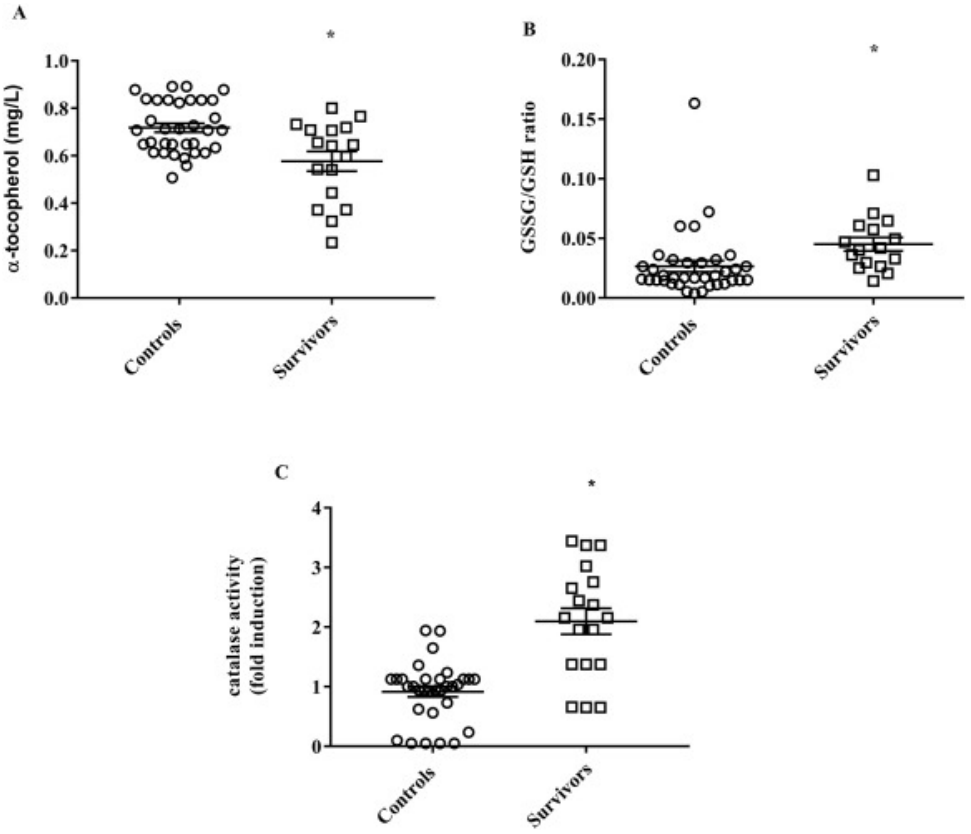

Fig. 2. Oxidative stress and inflammatory markers. Levels of NAPDH-oxidase (A), p65 (B), NLRP3 inflammasome (C) and GSDM-D (D) in PBMC of HL survivors and Controls. *p < 0.05; **p < 0.01.

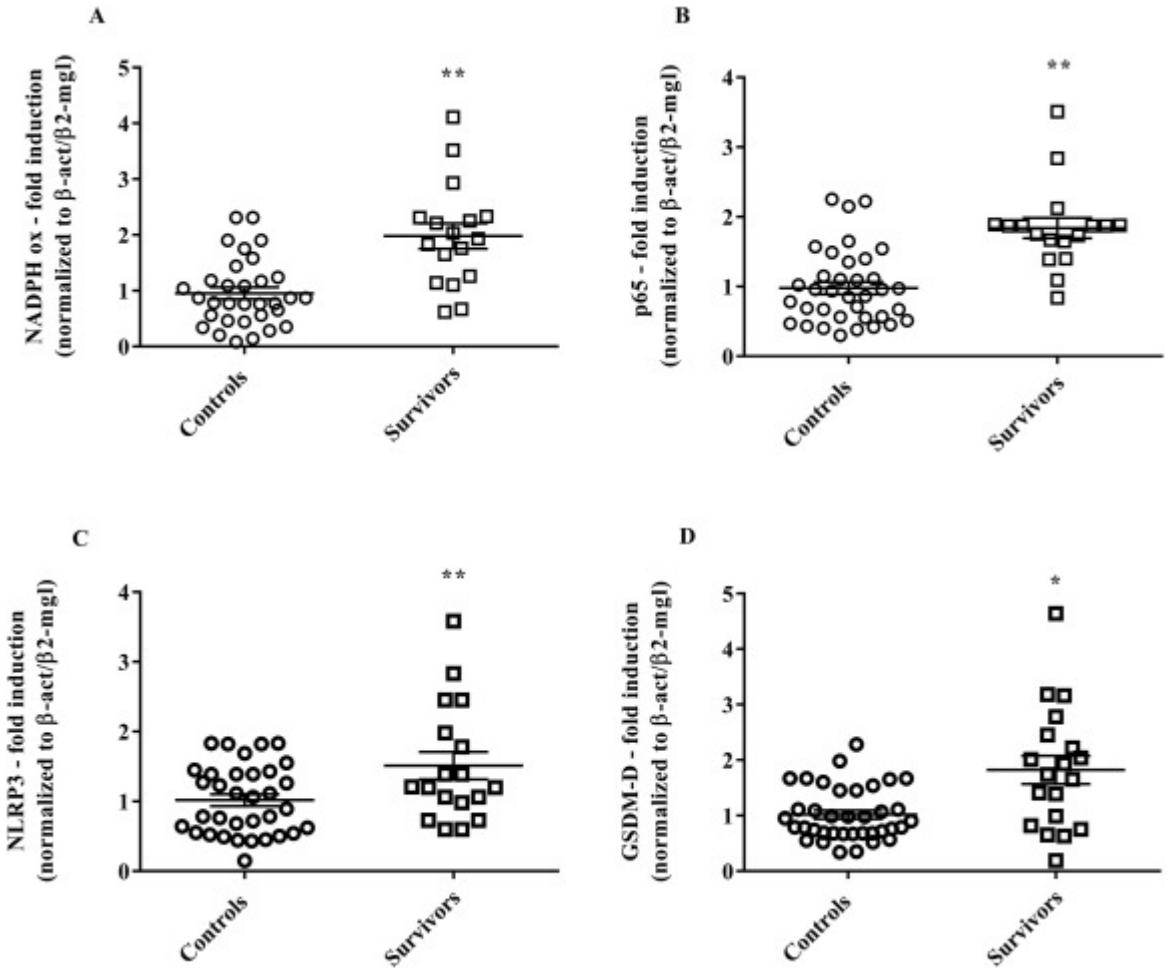

Fig. 3. Oxidative stress and inflammatory markers. Western blot analyses of NAPDH-oxidase (A), p65 (B), NLRP3 inflammasome (C) and GSDM-D (D) in PBMC of HL survivors and Controls. *p < 0.05.

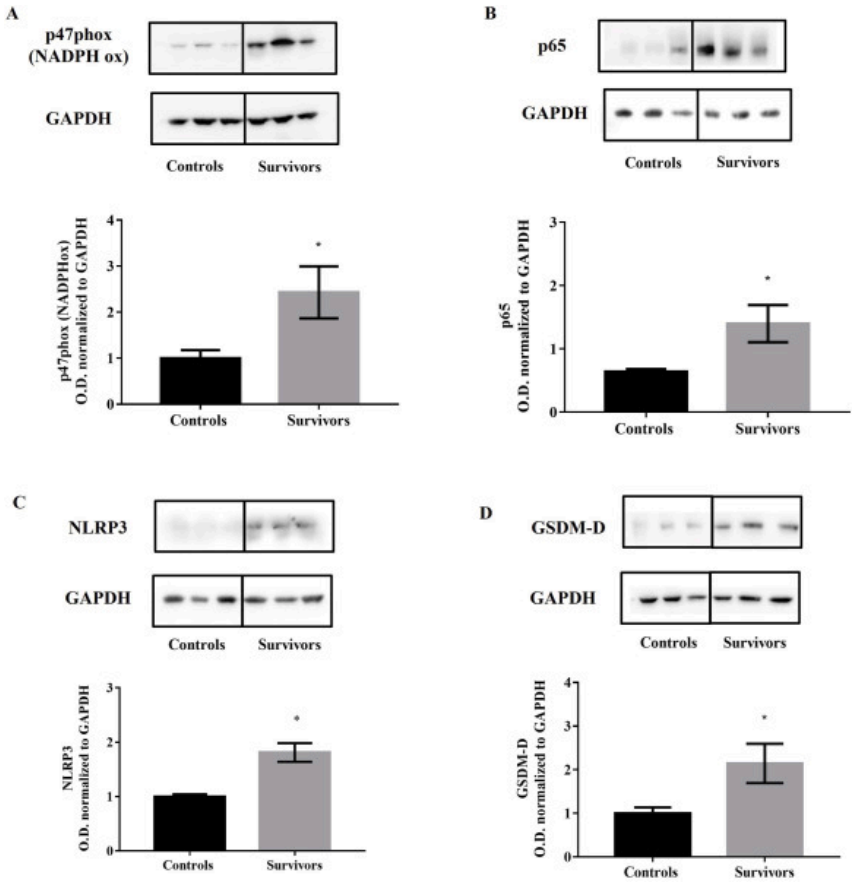

Fig. 4. Interleukin-6 (A) and Interleukin-1β (B) expression in PBMC of HL survivors and Controls. *p < 0.05; ****p < 0.0001.

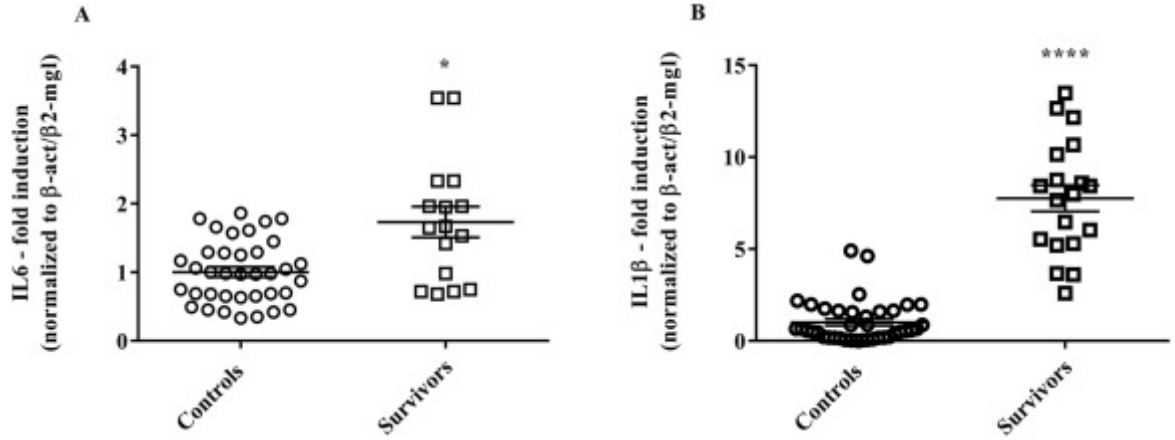

Fig. 5. AGEs and sRAGE. CML (A), MG-H1 (B) and sRAGE (C) levels in plasma of HL survivors and Controls. *p < 0.05; **p < 0.01.

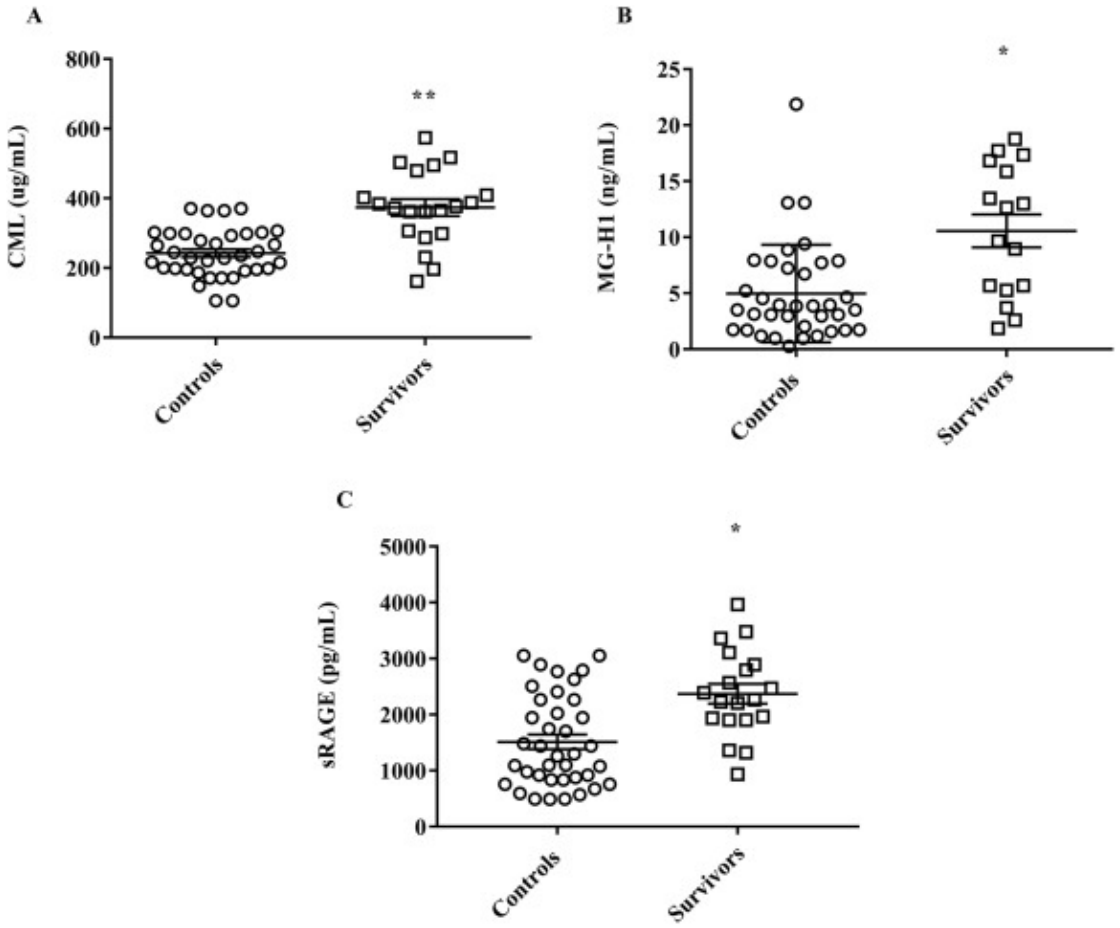

Fig. 6. Expression of RAGE (A) **and AGER1 (OST-48)** (B) in PBMC of HL survivors and Controls. **p < 0.01.